

Los Alamos National Laboratory is operated by the University of California for the United States Department of Energy under contract W-7405-ENG-36.

TITLE: THE THREE-DIMENSIONAL HYDRODYNAMIC HOT-SPOT MODEL

LA-UR--85-742

AUTHOR(S): Charles L. Mader, T-14
James D. Kershner, T-14

DE85 009587

MASTER

SUBMITTED TO: Eighth Symposium (International) on Detonation
Albuquerque, NM
July 15-19, 1985

DISCLAIMER

This report was prepared as an account of work sponsored by an agency of the United States Government. Neither the United States Government nor any agency thereof, nor any of their employees, makes any warranty, express or implied, or assumes any legal liability or responsibility for the accuracy, completeness, or usefulness of any information, apparatus, product, or process disclosed, or represents that its use would not infringe privately owned rights. Reference herein to any specific commercial product, process, or service by trade name, trademark, manufacturer, or otherwise does not necessarily constitute or imply its endorsement, recommendation, or favoring by the United States Government or any agency thereof. The views and opinions of authors expressed herein do not necessarily state or reflect those of the United States Government or any agency thereof.

By acceptance of this article, the publisher recognizes that the U.S. Government retains a nonexclusive, royalty-free license to publish or reproduce the published form of this contribution, or to allow others to do so, for U.S. Government purposes.

The Los Alamos National Laboratory requests that the publisher identify this article as work performed under the auspices of the U.S. Department of Energy.

Los Alamos Los Alamos National Laboratory
Los Alamos, New Mexico 87545

THE THREE-DIMENSIONAL HYDRODYNAMIC HOT-SPOT MODEL

Charles L. Mader and James D. Kershner
Los Alamos National Laboratory
Los Alamos, New Mexico

The interaction of a shock wave with a single air hole and a matrix of air holes in PETN, HMX, and TATB has been numerically modeled. The hot-spot formation, interaction, and the resulting build up toward detonation were computed using three-dimensional numerical Eulerian hydrodynamics with Arrhenius chemical reaction and accurate equations of state according to the hydrodynamic hot-spot model. The basic differences between shock sensitive explosives (PETN, HMX) and shock insensitive explosives (TATB, NQ) may be described using the hydrodynamic hot-spot model. The reactive hydrodynamics of desensitization of heterogeneous explosives by a weak preshock has been numerically modeled. The preshock desensitizes the heterogeneous explosive by closing the air holes and making it more homogeneous. A higher pressure second shock has a lower temperature in the multiple shocked explosive than in single shocked explosive. The multiple shock temperature may be low enough to cause a detonation wave to fail to propagate through the preshocked explosive.

INTRODUCTION

A shocked homogeneous explosive such as nitromethane first completely decomposes at the piston-explosive interface and achieves a detonation with a peak pressure that builds up toward the C-J pressure of the high-density shocked nitromethane. The detonation wave overtakes the shock wave, and the pressure at the end of the reaction zone decays toward the piston pressure.¹

If one introduces gas bubbles or grit into a homogeneous explosive such as a liquid or a single crystal, thereby producing a heterogeneous explosive, the minimum shock pressure necessary to initiate propagating detonation can be decreased by one order of magnitude.

Heterogeneous explosives, such as PBX-9404 or PBX-9502, show a different behavior than homogeneous explosives show when propagating along confining surfaces. A heterogeneous explosive

can turn sharp corners and propagate outward, and depending upon its sensitivity, it may show either very little or such curvature when propagating along a metal surface. The mechanism of initiation for heterogeneous explosives is different from the simple Arrhenius kinetic model found adequate for homogeneous explosives.¹ Heterogeneous explosives are initiated and may propagate by the process of shock interaction with density discontinuities such as voids. These interactions result in hot regions that decompose and produce increasing pressures that cause more and hotter decomposing regions. The shock wave increases in strength, releasing more and more energy, until it becomes strong enough that all of the explosive reacts and detonation begins.

This process is described by the "hydrodynamic hot-spot" model, which models the hot-spot formation from the shock interactions that occur at density discontinuities and describes

FMB

the decomposition using the Arrhenius rate law and the temperature from the BOM equation of state.¹

The numerical modeling of the interaction of a shock wave with a single density discontinuity was reported in Ref. (1), where an 8.5-GPa shock interacting with a single spherical hole in nitromethane was studied. The study was extended to four rectangular holes.¹ It was determined that 0.0032-mm-radius cylindrical voids would build toward detonation and 0.001-mm-radius voids would form hot spots that failed to propagate because of rarefactions cooling the reactive wave.

The process of shock initiation of heterogeneous explosives has been investigated¹ numerically by studying the interaction of shock waves with a cube of nitromethane containing 91 holes. An 8.5-GPa shock interacting with a single 0.002-mm hole did not build toward detonation. When the shock wave interacted with a matrix of 0.002-mm holes, it became strong enough to build toward detonation. Reducing the size of the holes to 0.0004 mm resulted in a sufficient amount of the explosive decomposing to compensate for the loss in energy to the flow caused by the interaction of the shock wave with the holes. The shock wave slowly grew stronger, but it did not build to detonation in the time of the calculation.

A 5.5-GPa shock wave interacting with a matrix of 0.002-mm holes resulted in insufficient heating of the resulting hot spots to cause significant decomposition.

The process of desensitization by preshocking was found to be a result of the holes being closed by the low-pressure initial shock wave without resulting in appreciable explosive decomposition. The higher pressure shock that arrived later did not have holes with which to interact and behaved like a shock wave in a homogeneous explosive until it caught up with the lower pressure preshock wave.

The basic processes in the shock initiation of heterogeneous explosives have been numerically modeled in three dimensions. The interaction of a shock wave with density discontinuities, the resulting hot-spot formation, interaction, and the build up toward detonation or failure have been modeled. In this paper the hydrodynamic hot-spot model is used to investi-

gate other explosives and other kinetics to study the basic differences between shock sensitive and shock insensitive explosives.

It has been observed that preshocking a heterogeneous explosive with a shock pressure too low to cause propagating detonation in the time of interest can cause a propagating detonation in unshocked explosive to fail to continue propagating when the detonation front arrives at the previously shocked explosive. The resulting explosive desensitization was modeled using a Forest Fire decomposition rate that was determined only by the initial shock pressure of the first shock wave passing through the explosive.¹ This model could reproduce the experimentally observed explosive desensitization of TATB (triaminotrinitrobenzene) explosives previously shocked by short duration 25 and 50-kilobar pulses. It could not reproduce the observed results for low or high preshock pressures that fail to quench a propagating detonation.

To determine the mechanism of the explosive desensitization by preshocking, we used a three-dimensional reactive hydrodynamic model of the process. With the mechanism determined, it was possible to modify the decomposition rate to include both the desensitization and failure to desensitize effects.

NUMERICAL MODELING OF SHOCK SENSITIVITY

The three-dimensional Eulerian reactive hydrodynamic code JDE is described in Ref. (4). It uses techniques identical to those described in detail in Ref. (1) and used successfully for describing two-dimensional Eulerian flow with mixed cells and multicomponent equations of state and for modeling reactive flow. It has been used to study the interaction of multiple detonation waves,¹ the basic process in shock initiation of heterogeneous explosives,^{1,2} and the reactive hydrodynamics of a matrix of tungsten particles in HMX.³

The Arrhenius reactive rate law was used with the constants determined experimentally by Raymond M. Rogers and described in Ref. (1). The constants used are given in Table 1.

TABLE 1
Arrhenius Constants

Explosive	Activation Energy (kcal/mole)	Frequency Factor (sec^{-1})
Nitroguanidine	20.9	20.4
EMX	54.9	3.10×10^{13}
EMX	52.7	1.9×10^{13}
PETN	47.0	4.3×10^{13}

The BOM equation-of-state constants used for PETN are described in Ref. (1). The BKW detonation product and the solid equation-of-state constants used in the BOM equation of state are given in Ref. (6).

A constant velocity piston was applied to the bottom of the explosive cube, shocking the explosive initially to the desired pressure. When the shock wave interacts with a hole, a hot spot with temperatures several hundred degrees hotter than the surrounding explosive is formed in the region above the hole when it is collapsed by the shock wave. The hot region decomposes and contributes energy to the shock wave, which has been degraded by the hole interaction.

Whether this energy is sufficient to compensate for the loss from the hole interaction depends upon the magnitude of the initial shock wave, the hole size, and the interaction with the flow from nearest neighbor hot spots. The objective of the study was to investigate the nature of this complicated interaction and to determine if the hydrodynamic hot-spot model was adequate to describe the experimentally observed sensitivity to shock initiation of the heterogeneous explosives PETN, EMX, TATB, and Nitroguanidine with PETN being the most sensitive and Nitroguanidine the least sensitive.

For example, to initiate PBX-9404 (EMX-based explosive) or PBX-9502 (TATB-based explosive) at maximum pressed density within 4 mm of shock run requires a shock wave in PBX-9404 of 5 GPa and in PBX-9502 of 16 GPa as determined from the experimental Pop plots.⁸

To initiate PETN at 1.75 g/cm³ (crystal density is 1.778) within 4 mm of shock run requires a pressure of only 2 GPa, while to initiate Nitroguanidine at 1.723 g/cm³ (crystal density is 1.774) within 4 mm of shock run requires a pressure of 25 GPa.⁸

The hole size present in such pressed explosives varies from holes of 20 to 600 Å in the TATB crystals to holes as large as 0.5 mm in the explosive-binder matrix. Most of the holes vary in size from 0.05 to 0.005 mm in diameter, so we examined holes in that range of diameters.

As shown in Ref. (1), the hot spot formed when a shock wave interacts with a spherical hole scales with the radius of the hole as long as no chemical reaction occurs. Using hot-spot temperatures in the calculated range of 700 to 1300 K and calculating the adiabatic explosion times, one observes the ordering according to sensitivity (time to explosion) shown in Table 2. The ordering is identical to that observed experimentally.

TABLE 2
Hot-Spot Explosion Times

Explosive	Hot-Spot Temperature		
	700 K	1000 K	1300 K
Nitroguanidine	1500 μs	120 μs	10 μs
EMX	1200 μs	1.5×10^{-1} μs	1.5×10^{-2} μs
EMX	120 μs	1.5×10^{-1} μs	1.5×10^{-2} μs
PETN	100 μs	1.5×10^{-1} μs	1.5×10^{-2} μs

The interaction of shock waves of various pressures with single cubical air holes of various sizes in PETN, EMX, TATB, and NQ was investigated. The calculations model the hot-spot explosion and failure to propagate because of rarefactions cooling the reactive wave. If the reaction becomes too fast to numerically resolve the cooling by rarefactions, the flow builds toward a detonation too quickly.

A summary of the results of the study is shown in Table 3. The ordering of shock sensitivity of the explosives is again observed experimentally correlating well with the observed Pop plot data.⁸

To evaluate the sensitivity to shock more realistically, we studied the interaction of a 5-GPa shock wave in EMX with a matrix of spherical holes of 4×10^{-3} -mm diameter. The computational grid contained 24 x 22 by 36 cells, each 1×10^{-3} mm on a side. The 36 air holes were described by 4 cells per sphere diameter. Numerical tests with 2 to 6 cells per sphere diameter showed the results were independent of grid size for more than 3 cells per sphere diameter. The

air holes were located on a hexagonal close-packed lattice (HCP). The closest distance for the HCP matrix between holes was 3.8×10^{-3} mm. The time step was 1.0×10^{-8} μ s. The void fraction is 10%. While a single hole fails to build toward a detonation as shown in Fig. 1, the matrix of holes builds toward a detonation as shown in Fig. 2. The experimental run to detonation for a 5-GPa shock wave in 1.71 g/cm^3 EMX is 0.17 cm. While a propagating detonation would not be expected to occur experimentally in this geometry (the computed detonation is the result of insufficient numerical resolution to resolve the reaction at high pressures and temperature), the enhancement of the shock wave would occur.

TABLE I
Summary of Results for Various Cases

Explosive	Shock Pressure (GPa)	Void Fraction (%)	Result
EMX	1.0×10^{-3}	0	Failure to build toward a detonation
	1.0×10^{-3}	10	Failure to build toward a detonation
	1.0×10^{-3}	20	Failure to build toward a detonation
	1.0×10^{-3}	30	Failure to build toward a detonation
	1.0×10^{-3}	40	Failure to build toward a detonation
TATB	1.0×10^{-3}	0	Failure
	1.0×10^{-3}	10	Failure
	1.0×10^{-3}	20	Failure to build toward a detonation
	1.0×10^{-3}	30	Failure
PETN	1.0×10^{-3}	0	Failure to build toward a detonation
	1.0×10^{-3}	10	Failure to build toward a detonation
MCP	1.0×10^{-3}	0	Failure
	1.0×10^{-3}	10	Failure to build toward a detonation

The interaction of a 12.5-GPa shock wave in TATB with a single spherical hole of 4×10^{-3} -mm diameter is shown in Fig. 3. It fails to build toward a detonation. The interaction of a 12.5-GPa shock wave in TATB with a matrix of spherical holes of 4×10^{-3} -mm diameter with a void fraction of 10% is shown in Fig. 4. The flow builds toward a detonation. The experimental run to detonation for a 12.5-GPa shock wave in 1.71 g/cm^3 TATB is 0.30 cm. The computed detonation occurs too quickly because of insufficient numerical resolution when the shock wave is enhanced to high enough pressures and temperatures by the interacting hot spots.

The interaction of a 2.0-GPa shock wave in PETN with a single spherical hole of 4×10^{-3} -mm diameter was calculated. Build up toward a detonation did not occur. The interaction of a 2.0-GPa shock wave in PETN with a matrix of spherical holes of 4×10^{-3} -mm diameter with a void fraction of 10% was calculated. The flow

builds toward a detonation after the hot spots interact.

The experimental run toward detonation values are about the same for a 12.5-GPa shock wave interacting with TATB with 10% voids, for a 5.0-GPa shock wave interacting with EMX with 10% voids, and for a 2.0 GPa shock wave interacting with PETN with 10% voids.

The hydrodynamic hot-spot model describes the basic difference between shock sensitive and shock insensitive explosives. The interaction of a shock wave with air holes in PETN, EMX, TATB, and MQ, the resulting hot-spot formation, interaction, and the build up toward detonation or failure have been modeled. Increased hole size results in larger hot spots that decompose more of the explosive and add their energy to the shock wave and result in increased sensitivity of the explosive to shock. Increased number of holes also causes more hot spots that decompose more explosive and increase the sensitivity of the explosive to shock. The interaction between hole size and number of holes is complicated and requires numerical modeling for adequate evaluation of specific cases. The hole size can become sufficiently small (the critical hole size) that the hot spot is cooled by side rarefactions before appreciable decomposition can occur. Since increasing the number of holes while holding the percentage of voids present constant results in smaller holes, we have competing processes that may result in either a more or less shock sensitive explosive. If the hole size is below the critical hole size, then the explosive will become less sensitive with increasing number of holes of decreasing diameter.

To evaluate the potential shock sensitivity of an explosive for engineering purposes, one needs to determine experimentally the Arrhenius constants. One then calculates the adiabatic explosion times for several assumed hot-spot temperatures to determine the relative sensitivity of the explosive compared with explosives of known sensitivity. A more detailed evaluation can be obtained from calculations using the hydrodynamic hot-spot model.

STUDIES OF DESENSITIZATION BY PRESHOCKING

Dick⁹ performed a **PHIBEX** radiographic study of detonation waves in **PBX-9502** (95/5 Triaminotrinitrobenzene/Kel-F binder at 1.894 g/cm³) proceeding up a 6.5- by 15.0-cm block of explosive that was preshocked by a 0.635-cm steel plate moving at 0.08 (Shot 1698) or 0.046 cm/ μ s (Shot 1914). The static and dynamic radiograph for Shot 1698 are shown in Fig. 5. The preshocked **PBX-9502** explosive quenches the detonation wave as it propagates into the block of explosive.

To investigate the mechanism of explosive desensitization by preshocking, we again used the reactive hydrodynamic code, **3DE**.⁶

A constant velocity piston was applied to the bottom of **TATB** explosive cube shocking the explosive to the desired pressure. When a higher pressure second shock was to be introduced, the piston velocity was increased and other piston state values changed as appropriate for a multiple shock of the required pressure.

A single shock pressure of 290 kbars in **TATB** has a density of 2.8388 g/cm³, particle velocity of 0.21798 cm/ μ s, energy of 0.02376 mb cc/g, and temperature of 1396 °K. A second shock pressure of 290 kbars in **TATB** initially shocked to 40 kbars has a density of 2.878 g/cm³, energy of 0.017759 mb-cc/g, particle velocity of 0.2040 cm/ μ s, and temperature of 804.2 °K.

When a shock wave interacts with a hole, a hot spot with temperatures hotter than the surrounding explosive is formed in the region above the hole after it is collapsed by the shock wave. The hot region decomposes and contributes energy to the shock wave, which has been degraded by the hole interaction.

Whether this energy is sufficient to compensate for the loss from the hole interaction depends upon the magnitude of the initial shock wave, the hole size, and the interaction with the flow from nearest neighbor hot spots.

The interaction of a 40-kbar shock with a single 0.004-cm-diameter air hole in **TATB** was modeled. After 0.025 μ s, the 40-kbar shock had collapsed the hole and a 290-kbar shock

wave was introduced which passed through the 40-kbar preshocked region and overtook the 40-kbar shock wave.

The shock temperature in the bulk of the **TATB** and the adiabatic explosion times are given below:

First Shock (kbar)	40	290	40
Second Shock (kbar)			290
Temperature (°K)	362.5	1396	804.2
Explosion Time (μ s)	10 ¹⁰	10 ⁻⁶	3.85

The density and burn fraction surface contours are shown in Figs. 6 and 7 and the cross sections through the center of the hole are shown in Fig. 8.

The 40-kbar shock wave collapsed the hole and formed a small weak hot spot which was not hot enough to result in appreciable decomposition of the **TATB**.

The 290-kbar shock wave temperature was not hot enough to cause explosion during the time studied in the bulk of the explosive previously shocked to 40 kbars; however, the additional heat present in the hot spot formed by the 40-kbar shock wave after it interacted with the hole was sufficient to decompose some of the explosive after it was shocked by the 290-kbar wave.

Propagating detonation occurred immediately after the 290-kbar shock wave caught up with the 40-kbar preshock.

To investigate the effect of the interaction of a matrix of holes with a multiple shock profile, a matrix of 10% air holes located on a hexagonal close packed lattice in **TATB** was modeled. The spherical air holes had a diameter of 0.004 cm. The initial configuration is shown in Fig. 9. The three-dimensional computational grid contained 16 by 22 by 36 cells each 0.001 cm on a side. The time step was 0.0002 μ s. Figure 10 shows the density and mass fraction cross sections for a 40-kbar shock wave followed after 0.045 μ s by a 290-kbar shock wave interacting with a matrix of 10% air holes of 0.004-cm-diameter in **TATB**.

The preshock desensitized the explosive by closing the voids and made it more homogeneous. The higher pressure second shock wave proceeded through the preshocked explosive until it caught up with the preshock.

The three-dimensional modeling study demonstrated that the desensitization occurs by the preshock interacting with the holes and eliminating the density discontinuities. The subsequent higher pressure shock waves interact with a more homogeneous explosive. The multiple shock temperature is lower than the single shock temperature at the same pressure, which is the cause of the observed failure of a detonation wave to propagate in preshocked explosives for some ranges of preshock pressure.

The modification indicated by the three-dimensional study to the Forest Fire decomposition rate being limited by the initial shock pressure was to add the Arrhenius rate law to the Forest Fire rate.

The Forest Fire rate for TATB is shown in Fig. 11 along with the Arrhenius rate calculated using the temperatures from the HOM equation of state for the partially burned TATB associated with the pressure as determined by Forest Fire. We will proceed using a burn rate determined by Forest Fire limited to the initial shock pressure and the Arrhenius rate using local partially burned explosive temperatures.

The experimental geometries studied using PHERMEX shown in Fig. 5 were numerically modeled using a reactive hydrodynamic computer code, 2DL, that solves the Navier-Stokes equation by the finite difference techniques described in Ref. (1). The users manual for the 2DL code is described in Ref. (10). For explosives that have been previously shocked, Craig³ experimentally observed that the distance of run to detonation for several multiple shocked explosives was determined primarily by the distance after a second shock had overtaken the lower pressure shock wave (the preshock). To approximate this experimental observation, we programmed the calculation to use Forest Fire rates determined by the first shock wave or the rates determined by any subsequent release waves that result in lower pressures and lower decomposition rates. As suggested by the three-dimensional study, we added the Arrhenius rate using the local partially burned explosive temperatures. The HOM equation of state and Forest Fire constants used to describe PBX-9502 (X0290) are given in Ref. (1).

The calculated pressure and mass fraction contours for PHERMEX shot 1698 are shown in Fig. 12 along with the radiographic interfaces.

The 2DL calculation had 50 by 93 cells to describe the PBX-9502 and 50 by 5 cells to describe the steel plate. The mesh size was 0.2 cm and the time step was 0.04 μ s.

The PHERMEX shot was numerically modeled using various velocity steel plates. The results are shown in Table 4. The results agree with the experimental evidence that detonation wave failure occurs in preshocked TATB shocked by steel plates with velocities of 0.046 and 0.08 cm/ μ s.

TABLE 4
9502 Desensitization Calculations

Steel Plate Velocity (cm/ μ s)	Preshock Pressure (kbar)	Result Upon Arrival of Detonation Wave
0.320	9	Detonates preshocked \square
0.037	14	Failure in preshocked \square
0.045	23	Failure in preshocked \square
0.060	30	Failure in preshocked \square
0.100	70	Failure in preshocked \square
0.120	90	Detonates preshocked \square and after 1.8 cm run
0.160	130	Detonates preshocked \square
0.200	180	Detonates preshocked \square

The desensitization of heterogeneous explosive by preshocking may be attributed to the preshock closing the voids, thus making the explosive more homogeneous. The failure of a detonation wave to propagate in the preshocked explosive may be attributed to the lower temperature that occurs in the multiple shocked explosive than in the singly shocked explosive.

A rate law that combines the Forest Fire rate limited to the rate determined by the initial shock pressure and the Arrhenius rate law permits a description of multiple shocked explosive behavior for many engineering purposes.

REFERENCES

1. Charles L. Mader, Numerical Modeling of Detonations, University of California Press, Berkeley, 1979.
2. Charles L. Mader and James D. Kershner, "Three-Dimensional Modeling of Shock Initiation of Heterogeneous Explosives," Nineteenth Symposium (International) on Combustion, Williams and Wilkins, pp. 685-690, 1982.
3. Charles L. Mader, Richard D. Dick, "Explosive Desensitization by Pre-shocking," Internationale Jahrestagung, 1979. Combustion and Detonation Processes, pp. 569-579, 1979.
4. Charles L. Mader and James D. Kershner, "Three-Dimensional Eulerian Calculations of Triple-Wave Initiated PBX-9404," Los Alamos Scientific Laboratory Report LA 8206, 1980.
5. Charles L. Mader, "Detonation Wave Interactions," Seventh Symposium (International) on Detonation, pp. 669-677, NSWCMF82-334, 1981.
6. Charles L. Mader and James D. Kershner, "The Three-Dimensional Hydrodynamic Hot-Spot Model Applied to PETN, HMX, TATB, and NQ," Los Alamos National Report LA-10203-MS, 1984.
7. Charles L. Mader, James D. Kershner, and George H. Pimbley, "Three-Dimensional Modeling of Inert Metal-Loaded Explosives," Journal of Energetic Materials 1, pp. 293-324, 1983.
8. Terry R. Gibbs and Alphonse Popolato, LASL Explosive Property Data, University of California Press, Berkeley, 1980.
9. Charles L. Mader, LASL PHERMEX Data, Volume III, University of California Press, Berkeley, 1980.
10. James N. Johnson, Charles L. Mader, and Milton S. Shaw, "2DL: A Lagrangian Two-Dimensional Finite-Difference Code for Reactive Media," Los Alamos National Laboratory Report LA-8922 M, 1981.

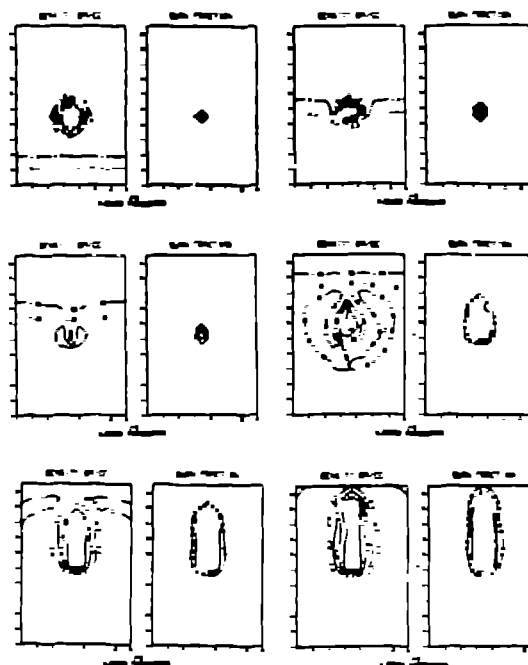


Fig. 1 - A 4×10^{-4} -mm diameter spherical air hole in HMX. The initial shock pressure is 5.0 GPa. The density and burn fraction cross sections through the center of the hole are shown at various times. It does not build toward detonation.

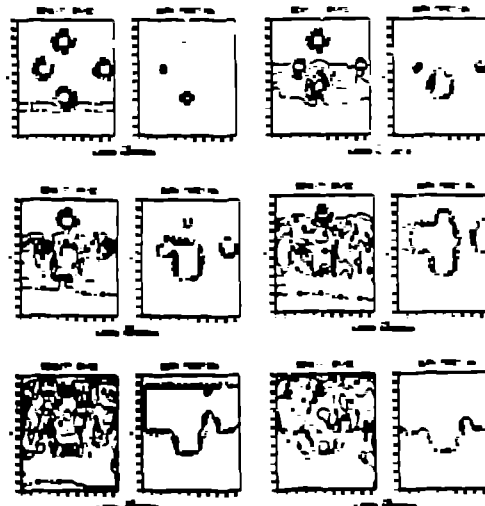


Fig. 2 - A matrix of 10% air holes in HMX. The spherical air holes have a diameter of 4×10^{-4} mm. The initial shock pressure is 5.0 GPa. The density and mass fraction contours are shown for a cross section through the center of the matrix. The flow builds toward a propagating detonation.

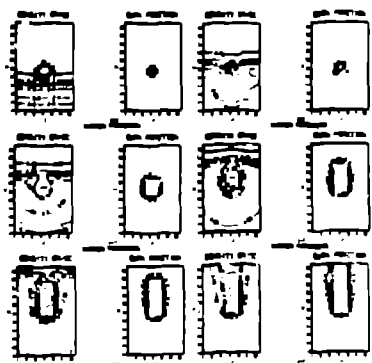


Fig. 3 - A 4×10^{-3} -mm diameter spherical hole in TNT. The initial pressure is 12.5 GPa. The density and burn fraction cross sections through the center of the hole are shown at various times. The flow does not build toward a detonation.

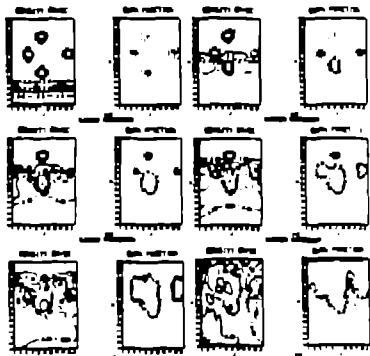


Fig. 4 - A matrix of 10% air holes in TNT. The spherical air holes have a diameter of 4×10^{-3} mm. The initial shock pressure is 12.5 GPa. The density and mass fraction contours are shown for a cross section through the center of the matrix. The flow builds toward a detonation.

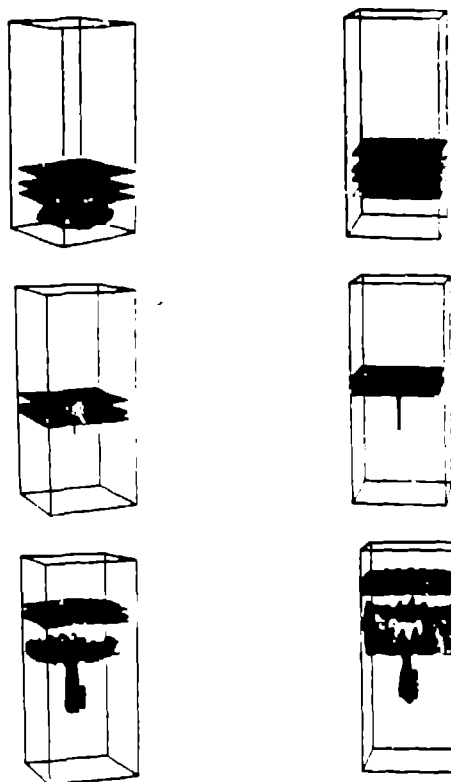


Fig. 6 - The density surface contours for a 40-kbar shock interacting with a single 0.004-cm-diameter air hole in TNT followed after 0.025 μ s by a 290-kbar shock wave.

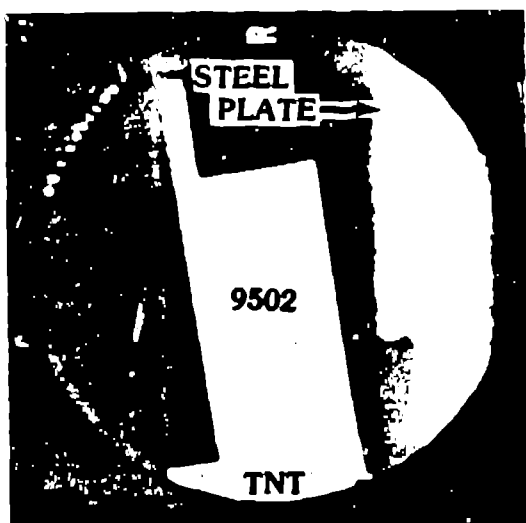


Fig. 5 - Static and dynamic radiograph 1698 of PRX-9502 shocked by a 0.635-cm-thick steel plate going 0.08 cm/ μ s and initiated by 2.54 cm of TNT and a P-40 lens.

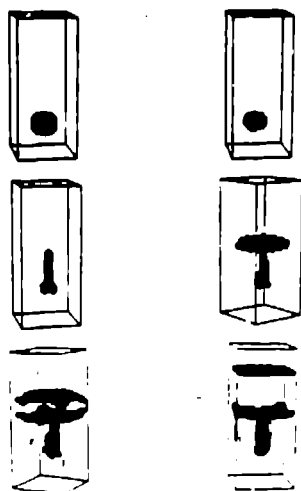


Fig. 7 - The burn fraction contours for the system shown in Fig. 6.



Fig. 8 - The density and burn fraction cross sections through the center of the hole for the system shown in Fig. 6.

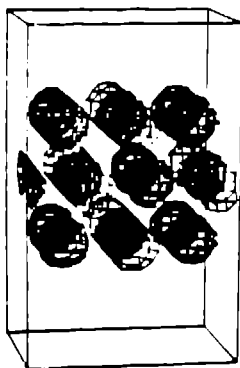


Fig. 9 - The initial configuration of a matrix of 10% air holes in TATB.



Fig. 10 - The density and mass fractions cross sections are shown for a 40-kbar shock wave followed after 0.045 μ s by a 290-kbar shock wave interacting with a matrix of 10% air holes of 0.004-cm-diameter in TATB.

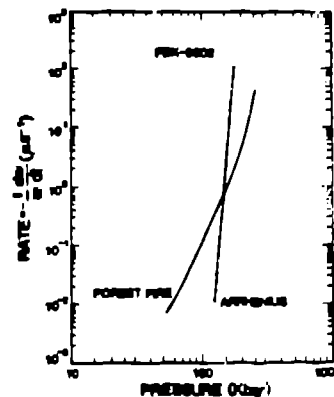


Fig. 11 - The burn rate as a function of pressure for the Forest Fire burn model and the Arrhenius rate law using the BOM temperatures associated with the Forest Fire pressures.

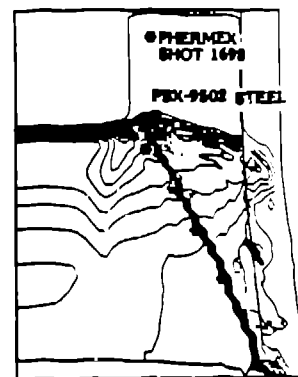


Fig. 12 - The pressure and mass fraction contours for a detonation wave in PEX-9502 interacting with explosive that had been previously shocked to 50 kbars. The PHERMEX radiograph interfaces are shown by stars. The mass fraction contour interval is 0.1 and shown as a thick almost solid line. The pressure contour interval is 40 kbars.